When, where, and how the corpus callosum changes in MCI and AD

A multimodal MRI study

M. Di Paola, PsyS
F. Di Iulio, PhD
A. Cherubini, PhD
C. Blundo, MD
A.R. Casini, MD, PhD
G. Sancesario, MD
D. Passafiume, PhD
C. Caltagirone, MD
G. Spalletta, MD, PhD

Address correspondence and reprint requests to Dr. Margherita Di Paola, Laboratory of Clinical and Behavioral Neurology, IRCCS Santa Lucia Foundation, Via Ardeatina 306, 00179 Rome, Italy
m.dipaola@hsantalucia.it

ABSTRACT

Background: The corpus callosum (CC) has been shown to be susceptible to atrophy in Alzheimer disease (AD) as a correlate of wallerian degeneration or retrogenesis. However, when and where these 2 mechanisms intervene is still unclear.

Methods: In 3 memory clinics, we recruited 38 patients with amnestic mild cognitive impairment (MCI), 38 patients with mild AD, and 40 healthy controls (HC). Combining voxel-based morphometry and diffusion tensor imaging, we investigated CC white matter (WM) density and fractional anisotropy (FA), radial diffusivity (DR), and axial diffusivity (DA).

Results: Compared with HC, patients with amnestic MCI showed reduced WM density in the anterior CC subregion; however, FA, DR, and DA did not differ between the 2 groups. Significant changes were found in patients with mild AD compared with HC in the anterior and posterior CC regions. These differences were evident in both voxel-based morphometry and diffusion tensor imaging analyses. Specifically, we found reduced callosal WM density in the genu, posterior body, and splenium; decreased FA and increased DR in the anterior CC subregion; and increased DA, with no difference in the FA, in the posterior CC subregion.

Conclusions: Callosal changes are already present in patients with amnestic mild cognitive impairment (MCI) and mild Alzheimer disease (AD). The precocious involvement of the anterior callosal subregion in amnestic MCI extends to posterior regions in mild AD. Two different mechanisms might contribute to the white matter changes in mild AD: wallerian degeneration in posterior subregions of the corpus callosum (suggested by increased axial diffusivity without fractional anisotropy modifications) and a retrogenesis process in the anterior callosal subregions (suggested by increased radial diffusivity without axial diffusivity modifications). *Neurology*® 2010;74:1136–1142

GLOSSARY

AD = Alzheimer disease; **ADRDA** = Alzheimer's Disease and Related Disorders Association; **CC** = corpus callosum; **CDR** = Clinical Dementia Rating; **DA** = axial diffusivity; **DARTEL** = Diffeomorphic Anatomic Registration Through Exponential Lie Algebra; **DR** = radial diffusivity; **DTI** = diffusion tensor imaging; **FLAIR** = fluid-attenuated inversion recovery; **FOV** = field of view; **FSL** = FMRIB Software Library; **FWE** = family-wise error; **HC** = healthy controls; **MCI** = mild cognitive impairment; **MMSE** = Mini-Mental State Examination; **NINCDS** = National Institute of Neurological and Communicative Disorders and Stroke; **ROI** = region of interest; **SE** = spin-echo; **TBSS** = Tract-Based Spatial Statistics; **TE** = echo time; **TI** = inversion time; **TR** = repetition time; **VBM** = voxel-based morphometry; **VOI** = volume of interest; **WM** = white matter.

The human corpus callosum (CC) is a crucial white matter (WM) structure providing communication between the 2 hemispheres of the brain. It has been suggested that the CC is particularly susceptible to atrophy in Alzheimer disease (AD).[1,2]

When analyzing brain structural changes in AD, it is essential to clarify region specificity, time dependence, and the mechanisms responsible for these modifications. How these callosal changes can be visualized depends strictly on which MRI technique is adopted. In the past, most CC studies were focused on region of interest (ROI) and voxel-based morphometry (VBM) techniques.[3] However, these macrostructural techniques may not be sensitive to myelin

Supplemental data at www.neurology.org

From the IRCCS Santa Lucia Foundation (M.D.P., F.D.I., A.C., C.C., G.S.), Rome; Department of Internal Medicine and Public Health (M.D.P., D.P.), University of L'Aquila, L'Aquila-Coppito; Department of Neuroscience and Memory Clinic (C.B.), San Camillo Hospital, Rome; Memory Clinic (A.R.C.), San Giovanni Addolorata Hospital, Rome; and Department of Neuroscience and Memory Clinic (G.S., C.C.), "Tor Vergata" University of Rome, Italy.

Study funding: Supported by the Italian Ministry of Health (RF.06-07-08 and RC 06-07-08-09/A to M.D.P.).

Disclosure: Author disclosures are provided at the end of the article.

and axon degeneration, which can be revealed by diffusion methods such as diffusion tensor imaging (DTI).[4-6]

In our previous macrostructural analysis of CC in amnestic mild cognitive impairment (MCI) and AD,[7] we found callosal atrophy in the anterior and posterior CC in severe AD, and less pronounced atrophy in mild AD and amnestic MCI. Here, we used 2 different techniques to investigate both macrostructural (Diffeomorphic Anatomic Registration Through Exponential Lie Algebra [DARTEL]–VBM) and microstructural (Tract-Based Spatial Statistics [TBSS]–DTI) WM changes in larger homogeneous samples of patients with amnestic MCI and mild AD compared with healthy controls (HC). Our main aims were 1) to identify where in the CC and when in the different stages of AD callosal changes can be detected and 2) to test the hypothesis that different mechanisms might be responsible for different region-specific callosal changes in these patients. The assumption was that multimodal MRI values might yield more definitive information about the underlying mechanisms of CC changes in AD.

METHODS Between September 2005 and January 2008, 60 patients with amnestic MCI and 60 patients with mild AD were consecutively recruited from 3 memory clinics in Rome, Italy, to participate in this case-control study. Patients with amnestic MCI were diagnosed using Petersen criteria.[8] In addition, all patients with amnestic MCI had Mini-Mental State Examination (MMSE)[9] scores ≥24 and Clinical Dementia Rating (CDR)[10] scale scores of 0.5. The diagnosis of AD was made in accordance with the National Institute of Neurological and Communicative Disorders and Stroke (NINCDS)–Alzheimer's Disease and Related Disorders Association (ADRDA) criteria.[11] All patients with AD had MMSE[9] scores ≥18 and a CDR[10] score of 1, corresponding to what is known as mild AD. Exclusion criteria are described in detail in the earlier study of Di Paola et al.[9] Out of these 120 patients, 6 were excluded because of claustrophobia, 9 were excluded because of technical difficulties with the radiologic examination, and 29 were excluded because of evidence of focal parenchymal abnormalities or signal hyperintensities. For this purpose, the images were visually inspected by a neuropsychologist expert in neuroimaging and by a neuroradiologist. Both were blind to the identity of the participants. White matter lesions were considered to be present if they were hyperintense on both fluid-attenuated inversion recovery (FLAIR) and T2-weighted images. We included only subjects who, according to both observers, had no lesions. The final clinical samples included 38 patients with amnestic MCI and 38 patients with mild AD (for details, see table 1).

Sixty HC volunteered to participate in this study. They were recruited from universities, community recreational centers, and hospital personnel. Normal controls were required to have MMSE[9] scores ≥24, no memory symptoms, and normal documented memory function on standardized memory tests. A detailed list of exclusion criteria is described in the earlier study of Di Paola et al.[9] Of the initial 60 volunteers, 10 had neuropsychological deficits, and 50 were considered potentially eligible to participate in the study. Four of these 50 subjects were excluded because they were unable to undergo the MRI examination as a result of claustrophobia, 3 were excluded because of technical difficulties with the radiologic examination, and 3 were excluded because of evidence of focal parenchymal abnormalities. Thus, the final HC sample included 40 individuals (for details, see table 1).

Standard protocol approval, registration, and patient consent. All participants (or their proxies when needed) provided written informed consent. Consent was obtained according to the Declaration of Helsinki, and the study was approved by the Santa Lucia Foundation Research Ethics Committee.

Clinical and neuropsychological assessment. Trained clinical neurologists interviewed the patients and their caregivers using the NINCDS-ADRDA criteria[11] for the diagnosis of AD and Petersen criteria[12] for the diagnosis of amnestic

Table 1 Sociodemographic and clinical characteristics of patients with mild Alzheimer disease, patients with amnestic mild cognitive impairment, and healthy controls

	Subject group			Statistic			Bonferroni post hoc comparison (*p*)		
	Mild AD (n = 38)	Amnestic MCI (n = 38)	HC (n = 40)	χ^2 or *F*	*df*	*p* Value	Amnestic MCI vs mild AD	Amnestic MCI vs HC	Mild AD vs HC
Male, n	26	26	26	0.139	2	0.933			
Age, mean ± SD, y	73.3 ± 8.2	70.3 ± 6.4	64.6 ± 8.3	12.86	2, 113	0.000	0.274	0.004	0.000
Educational level, mean ± SD, y	7.8 ± 4.4	10.5 ± 4.1	12.0 ± 4.4	9.26	2, 113	0.000	0.023	0.411	0.000
MMSE score				117.37	2,113	0.000	0.000	0.001	0.000
Mean ± SD	22.7 ± 2.7	27.6 ± 1.7	29.2 ± 1.2						
Range	18-28	24-30	25-30						
CDR value	1	0.5	0						

Abbreviations: AD = Alzheimer disease; CDR = Clinical Dementia Rating; HC = healthy controls; MCI = mild cognitive impairment; MMSE = Mini-Mental State Evaluation.

Table 2 Performance scores of patients with mild Alzheimer disease, patients with amnestic mild cognitive impairment, and healthy controls in individual cognitive domains[a]

Neuropsychological assessment	Mild AD (n = 38)	Amnestic MCI (n = 38)	Healthy controls (n = 40)
Mental deterioration battery			
Verbal task			
RIR	19.29 (6.82)	26.82 (6.83)	44.44 (8.61)
RDR	1.37 (1.73)	3.47 (2.85)	9.80 (3.05)
PVF	20.08 (9.56)	29.76 (10.37)	35.39 (10.25)
SC	10.60 (3.20)	16.40 (4.20)	20.39 (4.99)
Visuospatial task			
IVM	15.32 (4.61)	19.76 (1.42)	20.18 (2.42)
PM47	17.82 (5.56)	26.26 (3.94)	28.64 (5.70)
CD	7.42 (2.52)	10.26 (1.16)	10.15 (1.58)
CDL	56.18 (11.15)	65.18 (3.56)	66.62 (3.69)

Abbreviations: AD = Alzheimer disease; CD = copying drawings; CDL = copying drawings with landmarks; IVM = immediate visual memory; MCI = mild cognitive impairment; PM47 = Raven Progressive Matrices '47; PVF = phonological verbal fluency; RDR = Rey 15-word Delayed Recall; RIR = Rey 15-word Immediate Recall; SC = sentence construction.
[a]Data are mean (SD).

MCI. The accepted interrater reliability for the diagnosis was Cohen $\kappa > 0.80$.

The MMSE[9] was administered to obtain a global index of cognitive impairment. The effect of the cognitive impairment on functional daily activities was rated using the CDR scale.[10] To assess individual cognitive domain performances, we administered the Mental Deterioration Battery,[13] a standardized and validated neuropsychological battery that consists of 7 neuropsychological tests from which 8 performance scores can be derived. Of the 8 total scores, 4 pertain to the elaboration of verbal stimuli and 4 pertain to visuospatial material. The tests were selected to obtain information about the functioning of different cognitive domains: verbal memory, short-term visual memory, logical reasoning, language, simple and constructional praxis, and executive functions. Accepted interrater reliability for the neuropsychological scores was Cohen $\kappa > 0.80$. For further details, see table 2.

MRI data acquisition. All MRI data were acquired on a 3-T Allegra magnetic resonance system (Siemens, Erlangen, Germany) using a birdcage head coil. The measurements were taken in a single session and consisted of the following pulse sequences: 1) double weighted turbo spin-echo (SE) acquired in transverse planes (repetition time [TR] 4,500 milliseconds, echo times [TE] 12 and 112 milliseconds, field of view [FOV] 230 × 172 mm, matrix 320 × 240, slice thickness 5 mm, 24 slices; 2) FLAIR in the same planes as the SE sequence (TR/TE 8,500/109 milliseconds, inversion time [TI] 2,000; FOV 230 × 168 mm, matrix 256 × 256, slice thickness 5 mm, 24 slices); 3) T1-weighted 3-dimensional images were obtained with partitions acquired in the sagittal plane using a modified driven equilibrium Fourier transform sequence (TE/TR = 2.4/7.92 milliseconds, flip angle 15°, TI 910, isotropic voxels 1 mm^3); and 4) diffusion-weighted volumes acquired using SE echo-planar imaging (TE/TR = 89/8,500 milliseconds, bandwidth 2,126 Hz/vx, matrix size 128 × 128, 80 axial slices, voxel size 1.8 × 1.8 × 1.8 mm^3) with 30 isotropically distributed orientations for the diffusion-sensitizing gradients at a b-value of 1,000 $s \cdot mm^2$ and 6 b = 0 images. To increase the signal-to-noise ratio, scanning was repeated 3 times. We minimized movement by stabilizing the head with cushions and tape before scanning.

VBM-DARTEL analysis. Images were processed and analyzed using VBM[14,15] in the framework of statistical parametric mapping (SPM5; Wellcome Department of Imaging Neuroscience, University College, London, UK). For each subject, the images were checked for scanner artifacts and gross anatomical abnormalities by a neuroradiologist and a neuropsychologist expert in neuroimaging. Then, all volumes were manually reoriented to approximate the orientation to the ICBM-152 default SPM5 template to improve image registration accuracy. First, they were segmented into WM and gray matter. Then, the DARTEL toolbox was used to obtain a high-dimensional normalization protocol (for details, see appendix e-1 on the *Neurology*® Web site at www.neurology.org).

We performed an analysis of variance to compare each diagnostic group (i.e., HC, amnestic MCI, mild AD) with respect to WM density. Statistical outcomes were corrected for multiple comparisons using family-wise error (FWE) at $p < 0.05$. Only significant findings were mapped onto the default SPM5 WM a priori and restricted to findings located on the CC using a predefined 3-dimensional volume of interest (VOI). This callosal VOI was drawn by one of the authors (M.D.P.) on 3 sequential coronal slices of the mean WM image (i.e., based on the averaged, normalized WM partitions of all subjects included). Before this VOI was applied to the statistical maps, it was smoothed with an 8-mm gaussian kernel.

DTI analysis. Diffusion-weighted images were processed with the FMRIB Software Library (FSL) program. Image distortions, induced by eddy currents and head motion, in the DTI data were corrected by applying a full affine alignment of each image to the mean no-diffusion-weighted image. After corrections, DTI data were averaged and concatenated into 31 (1 B0 + 30 B1000) volumes. A diffusion tensor model was fit at each voxel, generating fractional anisotropy (FA), axial diffusivity (DA), and radial diffusivity (DR) maps. In this work, we defined DR as the average of the second and third eigenvalues of the diffusion tensor, whereas DA corresponded to the first eigenvalue.

We used TBSS[16] version 1.2, part of FSL, for the postprocessing and analysis of multisubject DTI data (for details, see appendix e-1).

To test for localized differences across groups, voxel-wise statistics were performed for each point on the common FA skeleton. A permutation-based approach[17] that accounts for FWEs was used to control for multiple comparisons. Specifically, permutation-based inference cluster size ($t > 1$, $p < 0.05$) was used to test whether FA was reduced in patients with mild AD compared with HC, and whether DR and DA were significantly increased.

The significant voxels from 3 midsagittal slices (Montreal Neurological Institute x = −1, 0, +1) were projected onto a 2-dimensional sagittal plane.

RESULTS

Sociodemographic characteristics. The 3 groups of participants differed significantly with respect to age and educational level (table 1). There was no gender difference among groups. Thus, age

Figure 1 Corpus callosum macrostructural changes in mild Alzheimer disease and amnestic mild cognitive impairment

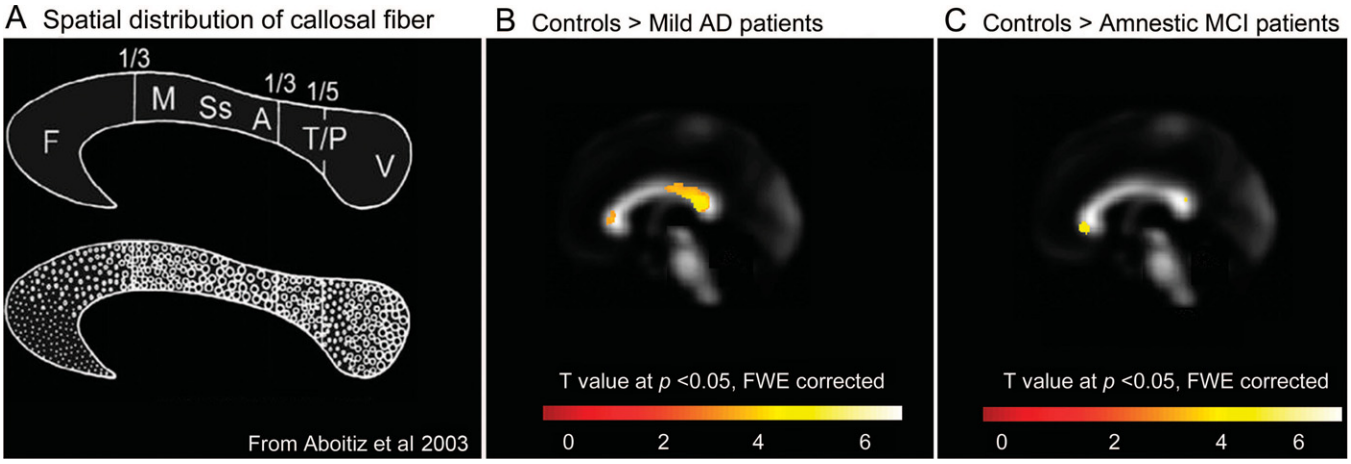

Illustrations of the spatial distribution of callosal fibers. (A). Group differences are illustrated for mild Alzheimer disease (AD) (B) and for amnestic mild cognitive impairment (MCI) (C) with respect to white matter density analyzed by voxel-based morphometry. The color bars encode the family-wise error (FWE)–corrected *p* value. F = frontal; M = motor; Ss = somatosensory; A = auditory; T/P = temporal/parietal; V = visual. Image reproduced from Aboitiz et al.,[41] with permission.

and education were entered as covariates in all statistical analyses to control for the effect of these variables on the main results.

VBM-DARTEL analysis. As shown in figure 1B, we found reduced WM density in the genu ($Z = 3.54$, FWE-corrected $p = 0.040$), posterior body, and splenium ($Z = 4.64$, FWE-corrected $p = 0.001$) of the CC in patients with mild AD compared with HC. When patients with amnestic MCI were compared with HC (figure 1C), we found reduced WM density only in the CC genu ($Z = 4.04$, FWE-corrected $p = 0.048$). We found no callosal WM density reduction in HC compared with the 2 patient groups.

DTI analysis. As shown in figure 2, the spatial distribution of differences ($p < 0.05$) between mild AD and HC in DTI parameters were as follows: A) DR was significantly greater in the entire CC in mild AD, B) DA was greater in the body and in the posterior subregion of the CC in mild AD, and C) FA was lower in the genu and anterior body of the CC in mild AD. No significant differences were found between amnestic MCI and HC.

DISCUSSION Our findings indicate that callosal structural changes in amnestic MCI and mild AD can be detected and localized precisely only using multimodal MRI.

The amnestic MCI group showed significant macrostructural atrophy only in the anterior callosal section. In the mild AD group, this atrophy extended to the posterior CC subsections and was accompanied by anterior and posterior microstructural modifications.

Regarding the amnestic MCI results, we previously described mild atrophy in the anterior subregion of the CC.[7] Furthermore, the present VBM results on mild AD agree with findings reported in several previously published ROI studies.[18,19]

Figure 2 Corpus callosum microstructural changes in mild Alzheimer disease

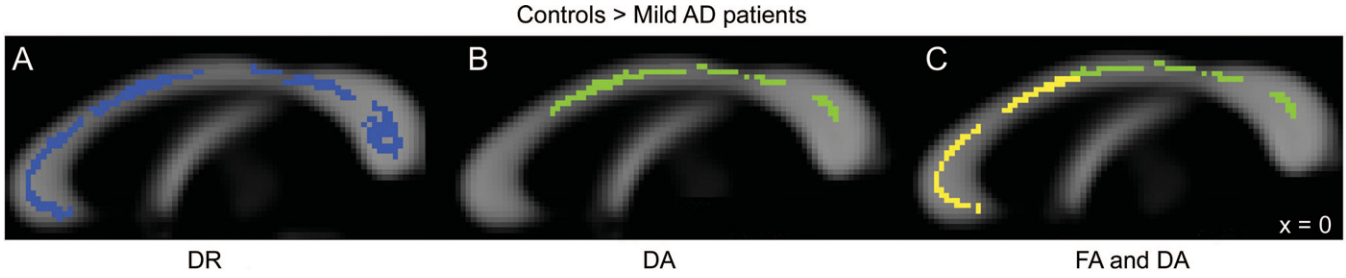

Compared with healthy controls, patients with mild Alzheimer disease (AD) show an increase in radial diffusivity (DR) in the entire corpus callosum (CC) (A), an increase in axial diffusivity (DA) in the midbody and posterior CC subregions (B), and a decrease in fractional anisotropy (FA) in the anterior CC subregion (C). All results are at the family-wise error–corrected *p* level. The DR, DA, and FA values are projected on a 2-dimensional sagittal plane.

The real innovation in this study was the simultaneous use of different DTI parameters (FA, DR, and DA), which allowed us to study the intrinsic differences in the callosal WM changes of our patients and to hypothesize different underlying mechanisms. FA measures the directionality of water diffusion. Recently, Choi et al.[20] investigated DR and DA, which measure diffusion perpendicular or parallel to the WM fibers. The assumption arising from experiments using animal models[20,21] is that significantly reduced DR in WM without differences in DA might indicate specifically compromised myelin integrity in the absence of axonal structural irregularities. Thus, taken together, these different diffusivity measurements should help us to understand the different mechanisms underlying microstructural callosal changes. Two of these mechanisms have already been described. The first, wallerian degeneration, assumes that callosal fiber change reflects atrophy of the corresponding cerebral cortex along the posterior anterior direction (from temporal-parietal to frontal lobes). The second, the retrogenesis hypothesis,[22] assumes that late-myelinating fibers, such as those in the genu, are more susceptible to myelin breakdown than earlier myelinating fibers, such as those in splenium, which are more resistant to retrogenesis.

In agreement with previous DTI studies in AD,[5,23,24] we found microstructural involvement of the anterior callosal WM expressed by decreased FA values. However, DR and DA measures indicated a more complex pattern. Indeed, in the anterior CC the preferential loss of water diffusion in the fiber direction (decreased FA) was accompanied by major diffusion in the direction perpendicular to the CC fibers (increased DR). Differently, in the posterior CC subregion we found increased water diffusion only in the direction of the fibers (increased DA, no difference in FA). A change in DR, not mirrored by a similar change in DA in the anterior portion of the CC, is most likely caused by specific damage to myelin sheaths that restrict DR. Thus, these changes suggest a loss of myelin integrity, possible due to the mechanism of retrogenesis. Differently, increased DA without FA modifications in the posterior CC subregion suggests widespread tissue damage resulting in a generalized increase in extracellular space due, for example, to the axonal atrophy expected in wallerian degeneration. Thus, wallerian degeneration could explain the atrophy in the posterior CC and the retrogenesis hypothesis could explain the changes in the anterior CC in AD.

Some other mechanisms have been suggested to explain CC atrophy in dementia, such as deterioration of cerebral hemodynamics and subsequent ischemic damage with extensive WM lesions.[25,26] However, this hypothesis is not applicable to our data because the subjects included in the present study had no WM lesions. Thus, although involvement of wallerian degeneration and retrogenesis in CC changes is just one possible explanation, it is the one most consistent with our findings.

Another issue concerns the partial lack of consistency between VBM and DTI data in MCI and AD. This can be explained by different, although partially overlapping, biologic underpinnings of volumetric and diffusivity variations. Indeed, the former is a measure of macroscopic structural characteristics, and the latter is sensitive to structural variations at the cellular and molecular level. Thus, the effects of fiber structure deterioration may produce different effects at different spatial scales, and results obtained from the 2 MRI techniques cannot be perfectly specular. This might be more evident in patients with dementia than in healthy individuals in which an anterior-posterior direction of microstructural change in CC has been reported.[27,28] Our results were the same, regardless of the method used, with the precocious anterior CC change in amnestic MCI extending posteriorly in mild AD. Reduced FA in the anterior portion of the CC has also been reported in normal aging,[29] in agreement with our present data on pathologic aging (i.e., mild AD). Nevertheless, we did not find callosal microstructural changes in amnestic MCI. To explain this partial incongruence between physiology and pathology, we speculate that many factors, some still unknown, might take part in the pathologic process of change. Consequently, the amnestic MCI/AD data discrepancy, already present when different MRI techniques are applied, might be amplified in comparisons with the physiologic changes in healthy subjects. These considerations highlight the importance of using multimodal MRI techniques to measure different parameters when investigating pathophysiologic changes in the brain.

This study differs from previous research for several reasons, which might partially explain the discrepant findings. Here, we recruited homogeneous groups of patients with mild AD or amnestic MCI. In all VBM studies[2,15,30,31] and most DTI studies,[32,33] patients with AD who had mixed disease severity were recruited. Another issue concerns the intrinsic limitations of the techniques, such as the different modalities for implementing VBM, which influence intergroup morphometric comparisons.[34,35] In the present study, we used the DARTEL-VBM approach[36] implemented in SPM5. This technique overcomes the limits of previous VBM preprocessing by using better registration and by creating an iterative template. Another issue concerns the DTI technique. The variability of results can be explained by

the size and the placement of ROIs across studies. Furthermore, the VBM-style approach in DTI studies[24,37] presents problems primarily related to image registration and smoothing.[16,38] The TBSS,[39,40] used here, seems to overcome the limitations due to the alignment of FA images from multiple subjects and to the arbitrariness of the choice of spatial smoothing extent.

Our results, obtained using a case-control design comparing HC, MCI, and AD, should be further investigated in a longitudinal study of healthy subjects at high risk of developing AD (e.g., carriers of the ApoE ε4 gene or with AD familiarity) and in patients with the earliest clinical manifestations of dementia (amnestic MCI).

DISCLOSURE

Dr. Di Paola, Dr. Di Iulio, and Dr. Cherubini receive research support from the Italian Ministry of Health. Dr. Blundo, Dr. Casini, Dr. Sancesario, and Dr. Passafiume report no disclosures. Dr. Caltagirone has served on scientific advisory boards for Wyeth and Novartis; and has received research support from the Italian Ministry of Health. Dr. Spalletta receives research support from the Italian Ministry of Health.

Received September 8, 2009. Accepted in final form January 28, 2010.

REFERENCES

1. Zhang Y, Schuff N, Jahng GH, et al. Diffusion tensor imaging of cingulum fibers in mild cognitive impairment and Alzheimer disease. Neurology 2007;68:13–19.
2. Li S, Pu F, Shi F, Xie S, Wang Y, Jiang T. Regional white matter decreases in Alzheimer's disease using optimized voxel-based morphometry. Acta Radiol 2008;49:84–90.
3. Di Paola M, Spalletta G, Caltagirone C. In vivo structural neuroanatomy of corpus callosum in Alzheimer's disease and mild cognitive impairment using different MRI techniques: a review. J Alzheimers Dis Epub 2010 Feb 17.
4. Chua TC, Wen W, Slavin MJ, Sachdev PS. Diffusion tensor imaging in mild cognitive impairment and Alzheimer's disease: a review. Curr Opin Neurol 2008;21:83–92.
5. Ukmar M, Makuc E, Onor ML, Garbin G, Trevisiol M, Cova MA. Evaluation of white matter damage in patients with Alzheimer's disease and in patients with mild cognitive impairment by using diffusion tensor imaging. Radiol Med 2008;113:915–922.
6. Smith CD, Chebrolu H, Andersen AH, et al. White matter diffusion alterations in normal women at risk of Alzheimer's disease. Neurobiol Aging Epub 2008 Sep 16.
7. Di Paola M, Luders E, Di Iulio F, et al. Callosal atrophy in mild cognitive impairment and Alzheimer's disease: different effects in different stages. Neuroimage 2010;49:141–149.
8. Petersen RC, Doody R, Kurz A, et al. Current concepts in mild cognitive impairment. Arch Neurol 2001;58:1985–1992.
9. Folstein MF, Folstein SE, McHugh PR. "Mini-Mental State": a practical method for grading the cognitive state of patients for the clinician. J Psychiatr Res 1975;12:189–198.
10. Hughes CP, Berg L, Danziger WL, Coben LA, Martin RL. A new clinical scale for the staging of dementia. Br J Psychiatry 1982;140:566–572.
11. McKhann G, Drachman D, Folstein M, Katzman R, Price D, Stadlan EM. Clinical diagnosis of Alzheimer's disease: report of the NINCDS-ADRDA Work Group under the auspices of Department of Health and Human Services Task Force on Alzheimer's Disease. Neurology 1984;34:939–944.
12. Petersen RC, Smith GE, Waring SC, Ivnik RJ, Tangalos EG, Kokmen E. Mild cognitive impairment: clinical characterization and outcome. Arch Neurol 1999;56:303–308.
13. Carlesimo GA, Caltagirone C, Gainotti G. The Mental Deterioration Battery: normative data, diagnostic reliability and qualitative analyses of cognitive impairment. The Group for the Standardization of the Mental Deterioration Battery. Eur Neurol 1996;36:378–384.
14. Ashburner J, Friston KJ. Voxel-based morphometry: the methods. Neuroimage 2000;11:805–821.
15. Good CD, Johnsrude IS, Ashburner J, Henson RN, Friston KJ, Frackowiak RS. A voxel-based morphometric study of ageing in 465 normal adult human brains. Neuroimage 2001;14:21–36.
16. Smith SM, Jenkinson M, Johansen-Berg H, et al. Tract-based spatial statistics: voxelwise analysis of multi-subject diffusion data. Neuroimage 2006;31:1487–1505.
17. Nichols TE, Holmes AP. Nonparametric permutation tests for functional neuroimaging: a primer with examples. Hum Brain Mapp 2002;15:1–25.
18. Teipel SJ, Bayer W, Alexander GE, et al. Regional pattern of hippocampus and corpus callosum atrophy in Alzheimer's disease in relation to dementia severity: evidence for early neocortical degeneration. Neurobiol Aging 2003;24:85–94.
19. Wang PJ, Saykin AJ, Flashman LA, et al. Regionally specific atrophy of the corpus callosum in AD, MCI and cognitive complaints. Neurobiol Aging 2006;27:1613–1617.
20. Choi SJ, Lim KO, Monteiro I, Reisberg B. Diffusion tensor imaging of frontal white matter microstructure in early Alzheimer's disease: a preliminary study. J Geriatr Psychiatry Neurol 2005;18:12–19.
21. Sun SW, Song SK, Harms MP, et al. Detection of age-dependent brain injury in a mouse model of brain amyloidosis associated with Alzheimer's disease using magnetic resonance diffusion tensor imaging. Exp Neurol 2005;191:77–85.
22. Reisberg B, Franssen EH, Hasan SM, et al. Retrogenesis: clinical, physiologic, and pathologic mechanisms in brain aging, Alzheimer's and other dementing processes. Eur Arch Psychiatry Clin Neurosci 1999;249(suppl 3):28–36.
23. Shim YS, Yoon B, Shon YM, Ahn KJ, Yang DW. Difference of the hippocampal and white matter microalterations in MCI patients according to the severity of subcortical vascular changes: neuropsychological correlates of diffusion tensor imaging. Clin Neurol Neurosurg 2008;110:552–561.
24. Teipel SJ, Stahl R, Dietrich O, et al. Multivariate network analysis of fiber tract integrity in Alzheimer's disease. Neuroimage 2007;34:985–995.
25. Teipel SJ, Hampel H, Alexander GE, et al. Dissociation between corpus callosum atrophy and white matter pathology in Alzheimer's disease. Neurology 1998;51:1381–1385.
26. Tomimoto H, Lin JX, Matsuo A, et al. Different mechanisms of corpus callosum atrophy in Alzheimer's disease and vascular dementia. J Neurol 2004;251:398–406.

27. Sullivan EV, Pfefferbaum A. Diffusion tensor imaging and aging. Neurosci Biobehav Rev 2006;30:749–761.
28. Sullivan EV, Pfefferbaum A. Neuroradiological characterization of normal adult ageing. Br J Radiol 2007;80(spec no 2):S99–S108.
29. Sullivan EV, Rohlfing T, Pfefferbaum A. Quantitative fiber tracking of lateral and interhemispheric white matter systems in normal aging: relations to timed performance. Neurobiol Aging 2010;31:464–481.
30. Thomann PA, Wustenberg T, Pantel J, Essig M, Schroder J. Structural changes of the corpus callosum in mild cognitive impairment and Alzheimer's disease. Dement Geriatr Cogn Disord 2006;21:215–220.
31. Chaim TM, Duran FL, Uchida RR, Perico CA, de Castro CC, Busatto GF. Volumetric reduction of the corpus callosum in Alzheimer's disease in vivo as assessed with voxel-based morphometry. Psychiatry Res 2007;154:59–68.
32. Rose SE, Chen F, Chalk JB, et al. Loss of connectivity in Alzheimer's disease: an evaluation of white matter tract integrity with colour coded MR diffusion tensor imaging. J Neurol Neurosurg Psychiatry 2000;69:528–530.
33. Stahl R, Dietrich O, Teipel SJ, Hampel H, Reiser MF, Schoenberg SO. White matter damage in Alzheimer disease and mild cognitive impairment: assessment with diffusion-tensor MR imaging and parallel imaging techniques. Radiology 2007;243:483–492.
34. Keller SS, Wilke M, Wieshmann UC, Sluming VA, Roberts N. Comparison of standard and optimized voxel-based morphometry for analysis of brain changes associated with temporal lobe epilepsy. Neuroimage 2004;23:860–868.
35. Senjem ML, Gunter JL, Shiung MM, Petersen RC, Jack CR Jr. Comparison of different methodological implementations of voxel-based morphometry in neurodegenerative disease. Neuroimage 2005;26:600–608.
36. Ashburner J. A fast diffeomorphic image registration algorithm. Neuroimage 2007;38:95–113.
37. Medina D, DeToledo-Morrell L, Urresta F, et al. White matter changes in mild cognitive impairment and AD: a diffusion tensor imaging study. Neurobiol Aging 2006;27:663–672.
38. Jones DK, Symms MR, Cercignani M, Howard RJ. The effect of filter size on VBM analyses of DT-MRI data. Neuroimage 2005;26:546–554.
39. Damoiseaux JS, Smith SM, Witter MP, et al. White matter tract integrity in aging and Alzheimer's disease. Hum Brain Mapp 2009;30:1051–1059.
40. Zarei M, Damoiseaux JS, Morgese C, et al. Regional white matter integrity differentiates between vascular dementia and Alzheimer disease. Stroke 2009;40:773–779.
41. Aboitiz F, López J, Montiel J. Long distance communication in the human brain: timing constraints for interhemispheric synchrony and the origin of brain lateralization. Biol Res 2003;36:89–99.